

On an unverified nuclear decay and its role in the DAMA experiment

Josef Pradler,^{1,*} Balraj Singh,^{2,†} and Itay Yavin^{3,2,‡}

¹*Department of Physics and Astronomy, Johns Hopkins University, Baltimore, MD 21218, USA*

²*Department of Physics & Astronomy, McMaster University 1280 Main St. W, Hamilton, Ontario, Canada, L8S 4L8*

³*Perimeter Institute for Theoretical Physics 31 Caroline St. N, Waterloo, Ontario, Canada N2L 2Y5.*

The rate of the direct decay of ^{40}K to the ground state of ^{40}Ar through electron capture has not been experimentally reported. Aside from its inherent importance for the theory of electron capture as the only such decay known of its type (unique third-forbidden), this decay presents an irreducible background in the DAMA experiment. We find that the presence of this background, as well as others, poses a challenge to any interpretation of the DAMA results in terms of a Dark Matter model with a small modulation fraction. A 10 ppb contamination of natural potassium requires a 20% modulation fraction or more. A 20 ppb contamination, which is reported as an upper limit by DAMA, disfavors any Dark Matter origin of the signal. This conclusion is based on the efficiency of detecting ^{40}K decays as inferred from simulation. We propose measures to help clarify the situation.

I. INTRODUCTION

A ^{40}K concentration of 0.0117(1)% [1] in naturally occurring potassium, $^{\text{nat}}\text{K}$, is an ubiquitous source of radioactivity. Its decays in solidified rocks are responsible for the air's argon content and in a human body it is the element with one of the largest activities. The chemical similarity of sodium and potassium is not only responsible for a per mille fraction of $^{\text{nat}}\text{K}$ in seawater but may ultimately be the reason why trace amounts of potassium can also be found in ultra-radiopure scintillating crystals grown from NaI powders. These crystals are employed in rare event searches, such as in Dark Matter (DM) direct detection experiments where radioactive backgrounds pose one of biggest challenges limiting sensitivity.

The decay scheme of ^{40}K is shown in Fig. 1. All kinematically available energy levels in ^{40}Ar and ^{40}Ca are populated in the ^{40}K decay:

1. The dominant mode is the β^- decay to the calcium ground state with a half-life $T_{1/2}(\beta^-) = 1.407(7) \times 10^9$ yr and an endpoint energy of $Q_{\beta^-} = 1311.07(11)$ keV.
2. The argon branch is dominated by electron capture (EC) into the excited state $^{40}\text{Ar}^*(1460 \text{ keV})$ with $T_{1/2}(\text{EC}^*, 1460) = 11.90(11) \times 10^9$ yr. The nucleus subsequently de-excites by emission of a γ -ray.
3. Positron emission to the ground state of ^{40}Ar is possible. It has been measured [2] and found to have a small branching $\text{BR}_{\beta^+} = 0.00100(12)\%$.
4. Last but not least is EC directly into the ground state of ^{40}Ar . Little is known empirically about this decay and the current branching quoted in the

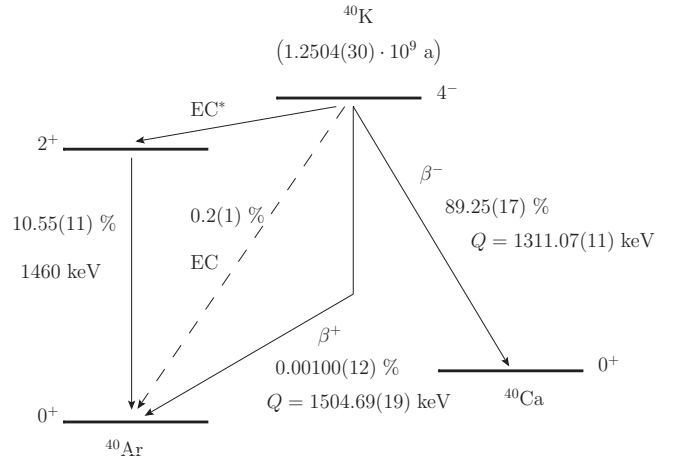


FIG. 1. Decay scheme of ^{40}K with numbers based on [1]. The dashed line depicts the direct decay to the ground state of ^{40}Ar for which no dedicated measurement has been reported. The branching ratio quoted is extracted from the measured β^+ decay rate and the extrapolated theoretical ratio EC/β^+ .

literature, $\text{BR}_{\text{EC}} = 0.2(1)\%$ [1], is based on the measurement of BR_{β^+} and a theoretical extrapolation from the EC to positron ratio for 1st and 2nd forbidden-unique transitions.

Experimentally, the most accessible modes are (1) and (2) because the respective electron or gamma-ray are readily detectable and numerous measurements exist. The quoted numbers are world-averages obtained in [3]. The observation of positron emission (3) is challenging because of its low intensity and pair-production background, but it was first reported in [2]. In contrast to the above modes, the rare EC to the ground state of ^{40}Ar in (4) has never been reported from a dedicated measurement. Since it is a transition from $J^\pi(^{40}\text{K}) = 4^-$ to $J^\pi(^{40}\text{Ar}) = 0^+$ it is classified as *unique third-forbidden* (3U) and it is the only such EC decay known [4, 5]. As such, its empirical verification would bring an important

* jpradler@pha.jhu.edu

† ndgroup@mcmaster.ca

‡ iyavin@perimeterinstitute.ca

closure to the theory of unique forbidden decays.

The energy release involved in this special decay is carried almost entirely by the emitted neutrino. Only about 3 keV of energy is observable from the Auger electron emission and the X-ray yield upon K-shell capture. As such, this decay forms an important irreducible background to the DAMA [6] experiment which looks for DM scattering in the laboratory. Since the experiment does not employ any discrimination between electron/gamma and nuclear-recoil activity, the release of only 3 keV associated with the rare EC decay of ^{40}K shows up directly in the region of interest for dark matter.

The purpose of this letter is to point out that—despite the omnipresent nature of ^{40}K —a dedicated measurement of one of its decay modes, namely the EC directly to the ground state of ^{40}Ar , remains outstanding. We begin by discussing what is currently known about this decay, carefully separating what is empirically established from what is based on a theoretical extraction. We then discuss the importance of this background in the DAMA experiment and how it affects the interpretation of the claimed results. We close with a brief discussion of how this special decay may be measured directly.

II. ^{40}K RARE EC DECAY

Given the absence of a reported measurement for the EC mode, its branching ratio, BR_{EC} , can be inferred from the theoretical ratio $\text{BR}_{\text{EC}}/\text{BR}_{\beta^+}$. The branching ratio of β^+ decay, BR_{β^+} , has been measured directly. The rationale behind this is that to leading order the atomic and nuclear pieces factorize and the branchings BR_{EC} and BR_{β^+} are dominated by the same nuclear matrix element, which then cancels in the ratio. Hence, the calculation of the ratio $\text{BR}_{\text{EC}}/\text{BR}_{\beta^+}$ becomes essentially a question of accurately modeling the atomic wave functions of the electron/positron and the neutrino involved.

Explicitly, the rate for positron emission is given by

$$\lambda_{\beta^+} \equiv \frac{\ln 2}{T_{1/2}(\beta^+)} = \frac{g^2}{2\pi^3} \int_0^{p_0} dp p^2 p_\nu^2 C_{3U}(Z_{\text{Ar}}, E), \quad (1)$$

where g is the Fermi constant times the cosine of the Cabibbo angle; $p(E)$ is the positron momentum (energy) with endpoint $p_0(E_0)$; the neutrino momentum is $p_\nu = E_0 - E$. The shape factor C_{3U} contains the nuclear matrix element \mathcal{M}_{3U} and the Coulomb correction in the form of the Fermi function $F(Z, E)$. The neutrino and positron are predominantly emitted in the triplet state allowing for one unit less in lepton orbital angular momentum when mediating a nuclear spin change of $J = 4$. Denoting by j_ν and j_e their respective angular momenta,

$$C_{3U} = g_A^2 |\mathcal{M}_{3U}|^2 R^6 \times \sum_{j_\nu, j_e} (\text{atomic part})_{j_\nu, j_e}, \quad (2)$$

where the sum is subject to the condition $j_\nu + j_e = J$; g_A is the axial vector coupling and R denotes the nuclear radius. We follow [7] in the evaluation of the atomic part.

Turning to EC, this process mainly occurs through K-shell capture and the rate is to a good approximation given by¹

$$\lambda_{\text{EC}} \equiv \frac{\ln 2}{T_{1/2}(\text{EC})} = \frac{g^2}{2\pi^3} f_K C_K, \quad (3)$$

where f_K contains the 1S amplitude for the bound state radial electron wave function and

$$C_K = \frac{q_K^6 R^6}{11025} \times g_A^2 |\mathcal{M}_{3U}|^2. \quad (4)$$

Here q_K is the momentum of the emitted neutrino. Equations (1) to (4) show that the nuclear matrix element and the strong sensitivity to the nuclear radius cancel in the ratio $\lambda_{\text{EC}}/\lambda_{\beta^+} = \text{BR}_{\text{EC}}/\text{BR}_{\beta^+}$. Using Eqs. (1) to (4) directly we find a value $\text{BR}_{\text{EC}}/\text{BR}_{\beta^+} = 190$ when using the atomic data collected in [8]. When using the approximations to the shape factor given in [9] we find a slightly smaller value of $\text{BR}_{\text{EC}}/\text{BR}_{\beta^+} = 150$.

Early evaluations [2] used $\lambda_{\text{EC}}/\lambda_{\beta^+} = 155$ without further reference to literature. The most recent one [1] uses

$$\frac{\lambda_{\text{EC}}}{\lambda_{\beta^+}} = 200(100) \Rightarrow \text{BR}_{\text{EC}} = 0.2(1) \%, \quad (5)$$

This is in good agreement with what we find using the direct calculation above, however it is important to note that this latter ratio is an extrapolated theoretical expectation and not computed from the above equations. The LOGFT computer program [10] used in nuclear data evaluations cannot compute the EC/ β^+ for the 3U ratio in (5). Instead the ratios to unique first- (1U) and second-forbidden (2U) transitions are calculated, $\text{BR}_{\text{EC}}/\text{BR}_{1U} = 8.51(9)$ and $\text{BR}_{\text{EC}}/\text{BR}_{2U} = 45.20(47)$, respectively. Assuming a constant increase by the same factor, $\text{BR}_{\text{EC}}/\text{BR}_{3U} = \text{BR}_{\text{EC}}/\text{BR}_{\beta^+} = 240$ is obtained from which the value in (5) has been adopted.

There is no doubt of the success of leading order theoretical predictions based on the V-A theory of weak interactions in explaining weak decay strengths and ratios observed throughout the periodic table. Yet, the ^{40}K decays to the ground states of ^{40}Ar and ^{40}Ca are the only known 3U transitions realized in nature [4, 5]. Hence, for the EC in question it is not obvious how to truly ensure the validity of (5), *e.g.* by gauging it against measurements of other 3U transitions. Theoretical attempts to match the calculated β^+ and β^- strengths to actual measurements yield discrepancies by a factor ~ 3 for $^{40}\text{K}(\beta^-)$ to ^{40}Ca and a factor ~ 6 for $^{40}\text{K}(\beta^+)$ to ^{40}Ar when simple nuclear shell models are employed [11]. These discrepancies are very likely the result of inaccuracies in the

¹ Higher shell captures contribute only about 10% to the total rate and yield energy depositions below the DAMA threshold. The error in the ratio induced by neglecting those contributions is much smaller than the overall uncertainty in this quantity.

evaluation of the corresponding nuclear matrix elements (which cancel when forming the ratio), but they make it difficult to feel confident about the theoretical estimation in Eq. (5). At the very least, they remind us of the importance of an empirical verification.

It is also possible to obtain a *theory-independent* estimate of BR_{EC} from measurements of the total half-life of ^{40}K . Indeed, this is facilitated by a recent high-precision measurement [12], $T_{1/2} = 1.248(9) \times 10^9 \text{ yr}$.² Neglecting positron emission we can write,

$$T_{1/2}^{-1}(\text{EC}) = T_{1/2}^{-1} - \left[T_{1/2}^{-1}(\beta^-) + T_{1/2}^{-1}(\text{EC}^*, 1460) \right],$$

and using the measured values for the β^- and EC^* branches one obtains,

$$\text{BR}_{\text{EC}} \equiv \frac{T_{1/2}}{T_{1/2}(\text{EC})} = 0.8(8) \%. \quad (6)$$

Given the large uncertainties it is clear that the available lifetime measurements are currently not sensitive enough to pin down the EC strength with reasonable accuracy. This special branch thus deserves its own dedicated measurement. Aside from its inherent significance, the precise activity of this branch also forms an important background in the DAMA experiment as we discuss in the following section.

III. POTASSIUM BACKGROUND IN DAMA

The DAMA experiment is situated in the Gran Sasso underground laboratory and searches for DM scattering off nuclei with a target made of 25 NaI(Tl) crystals amounting to almost 250 kg in mass [13]. The detector registers energy depositions between 2 keV to tens of MeV of almost any source: electrons, gamma- and X-rays, muons, alpha particles, and nuclear recoils. Events of the last class with recoil energies below a few keV_{ee} ³ are expected from the scattering of DM particles in the galactic halo against the target nuclei if the DM mass is $\gtrsim 10 \text{ GeV}$. Importantly, no discrimination procedure to veto against the other types of recoils is employed. Instead, the most compelling feature of the reported result is the annually modulating “single-hit”⁴ event rate between $2 - 6 \text{ keV}_{\text{ee}}$ with a phase that is compatible with

the phase expected from DM (June 2). The collaboration reports the *residual recoil rate* from which the average count rate of a cycle was subtracted.⁵ The residual rate exhibits an annually modulating pattern that can be nicely fitted to the model $S_m \cos \omega(t - t_0)$ with $\omega = 2\pi/(1 \text{ yr})$, a modulation amplitude of $S_m \simeq 0.04 \text{ cpd/kg}$ in the $2 - 4 \text{ keV}$ bin and a phase of $t_0 \approx 140 \text{ days}$. This is compatible with the expectation from a Maxwellian DM halo velocity distribution (see for example the recent review [14]).

However, knowledge of the modulated rate, S_m , without a detailed insight into the unmodulated rate, R_0 , makes the interpretation of the signal in terms of DM difficult. What is reported is that $R_0 \sim 1 \text{ cpd/kg/keV}$ for the spectrum below 10 keV . Essentially no information is available as to what it is comprised of. Radioactive backgrounds in rare event searches arise predominantly from naturally occurring radioactive isotopes (such as ^{40}K) in the detector material and its surroundings, from cosmogenically activated elements (*e.g.* ^{129}I), and from elements in the natural uranium (^{238}U) and thorium (^{232}Th) decay chains.

DAMA addresses all those background sources in [13] where they quote the concentrations of the different radio-isotopes. The main shortcoming of this study is that the influence on the low energy single-hit spectrum is not addressed quantitatively. The observed rate below 10 keV is essentially flat, with the exception of a bump around 3 keV . Flat spectra are typical for beta decays due to the Coulomb corrections at small electron emission energies as discussed below. Bumps in the keV energy region point towards EC. It has been speculated for a long time that the bump seen at 3 keV may very well be associated with K-shell electron capture of ^{40}K . The nuclear recoil in this decay is negligible and the scintillator detects the entire K-shell electron binding energy of ^{40}Ar (3.2 keV) released in the form of X-rays and Auger electrons. It is important to note that the position of the peak coincides with the maximum of S_m . Although the DAMA collaboration insists that these two bumps are of different origin, the presence of a poorly understood background in the signal region is at least unsettling.

Based on the reported levels of radioactivity, the authors of [16] were the first to try and evaluate the resulting rate in the DM signal region. Their main conclusion was that the unmodulated rate seems to require higher than reported concentrations of some of the isotopes. Moreover, in-situ contaminations of the crystals were found to dominate the low-energy spectrum as external radio-impurities are limited by the prominent backscatter peak they produce for $\gtrsim 40 \text{ keV}$. Fig. 2 shows the unmodulated “single-hit” spectrum: the three (red) line segments are reported event rates by DAMA [13]. The gray line is taken from [16] and shows the simulated

² Uncertainties in the decay scheme affect the error (but not the measured value) of $T_{1/2}$. This is because β^- -decay and EC are not registered with equal efficiencies. The error on BR_{EC} in (6) is calculated self-consistently which is also reflected by a larger adopted error on $T_{1/2}$ than what is originally quoted in [12].

³ Electron equivalent energy in keV.

⁴ “Single-hit” means that a prospective event must pass a coincidence veto with all other crystals. “Multiple-hit” events can, *e.g.*, be induced by γ -radiation accompanied by radioactive decay.

⁵ A DAMA cycle is very roughly one year but is subject to variations which are not further detailed by the collaboration.

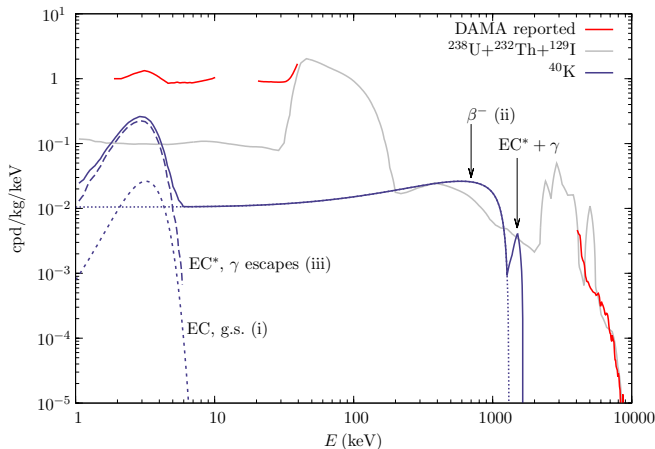


FIG. 2. DAMA “single-hit” spectrum and simulated backgrounds. The three disjoint pieces (in red) are DAMA reported rates from [13] and [15]. The statistical uncertainty in the signal region is negligible. The gray line is the spectrum from ^{129}I , ^{238}U , and ^{232}Th obtained in [16] with respective concentrations 0.2 ppt, 5 ppt, and 1.7 ppt. The blue lines show the various ^{40}K contributions as detailed in the text with a $^{\text{nat}}\text{K}$ contamination level of $c_K = 10$ ppb. The highest energy α -peak in the gray line is vetoed by the DAMA DAQ system [13].

spectrum from ^{238}U , ^{232}Th , and ^{129}I in-situ decays. The broad peak between 40 – 100 keV is from ^{129}I with little contribution elsewhere. Hence, the low-energy count rate is dominated by ^{238}U and ^{232}Th resulting in an essentially flat spectrum below 10 keV. The (quenched) α -decays in those chains result in peaks above 2 MeV, which are used by DAMA to derive the reported concentrations, but those are found to be insufficient to explain the observed rate below 10 keV. Though the contributed amount from ^{238}U and ^{232}Th at low energies is limited by the observation of the spectrum at high energies (\gtrsim few MeV), it is important to recognize that the contribution from ^{40}K decay is not similarly constrained.

DAMA reports an upper limit on the contamination level of $^{\text{nat}}\text{K}$ as $c_K \leq 20$ ppb [13]. They do so by using the decay of ^{40}K to the excited state of ^{40}Ar to look for double-coincidence events where the 3 keV is registered in one crystal and the 1460 keV gamma-ray is registered entirely in another crystal. The contamination level is obtained by dividing the observed double-coincidence rate by the probability for such events to occur. The latter was inferred from Monte Carlo (MC) simulation but no detailed description of this procedure has been provided. Given the indirect nature of the $^{\text{nat}}\text{K}$ determination and the lack of knowledge of potential systematic uncertainties, it may well be possible that the potassium contamination is larger than what is reported.

^{40}K contributes to the low energy spectrum in three distinct ways:

- i) The direct EC decay to the ground state of ^{40}Ar ,

which is the principal subject of this paper, contributes solely to the bump at 3.2 keV.

- ii) The electron emission associated with the ^{40}K to ^{40}Ca decay contributes a flat background that extends all the way up to the end-point energy of 1311 keV.
- iii) The EC decay to the excited state of ^{40}Ar results in the same low energy contribution to the 3 keV bump, but it is followed by the emission of 1460 keV gamma-ray. This decay contributes to the single-hit rate at low energy only when the 1460 keV gamma-ray escapes undetected.

The direct decay (i) is the easiest to calculate since it only depends on the contamination level of $^{\text{nat}}\text{K}$ in the NaI crystals and the branching ratio of this decay. If we assume a contamination level of c_K then the activity from ^{40}K decays to the ground state is given by,

$$\begin{aligned} \Gamma_{\text{EC}} &= c_{40} c_K \text{BR}_{\text{EC}} \frac{N_A \ln 2}{A_K T_{1/2} M_u}, \\ &= \frac{0.11}{\text{kg}_{\text{NaI}} \text{ day}} \left(\frac{\text{BR}_{\text{EC}}}{0.2\%} \right) \left(\frac{c_K}{20 \text{ ppb}} \right) \end{aligned} \quad (7)$$

Here N_A is Avogadro’s number, $M_u = 1 \text{ g/mol}$ is the molar mass constant, $T_{1/2}$ is the total lifetime of ^{40}K , $c_{40} = 0.0117(1)\%$ is the ^{40}K fraction in $^{\text{nat}}\text{K}$ [1], $A_K = 39.0983(1)$ is the atomic weight of potassium [17]; $c_K = 20$ ppb corresponds to the upper limit as reported by DAMA [13]. The decay will be perceived as a mono-energetic event at the ^{40}Ar K-shell binding energy of $E_K = 3.2 \text{ keV}$. The signal shape is hence dominated by the energy resolution of the detector $\sigma(\text{keV}) = 0.448\sqrt{E} + 0.0091E$ [13] where E is in units of keV. We find good agreement with the observed shape of the background and the total rate in the energy bin $[E_{\text{min}}, E_{\text{max}}]$ then reads

$$B_{\text{EC}} = \frac{\Gamma_{\text{EC}}}{2} \left[\text{Erf} \left(\frac{E_{\text{max}} - E_K}{\sqrt{2}\sigma} \right) - \text{Erf} \left(\frac{E_{\text{min}} - E_K}{\sqrt{2}\sigma} \right) \right]. \quad (8)$$

The β^- decay to ^{40}Ca , contribution (ii), is also easy to account for since the emitted electron is entirely contained in the crystal where the decay happened. Thus, the spectrum is found from the 3U shape factor for ^{40}Ca .⁶ At low energy this is a fairly flat background as shown in Fig 2. The shoulder present near the kinematical end-point of 1311 keV might offer a straightforward way to estimate the level of ^{40}K contamination level if it can be

⁶ The β^- spectrum shown in Ref. [16] is based on a GEANT4 simulation which erroneously computed the shape factor of an allowed decay. In Fig. 2 we have employed the correct shape factor. It mainly affects the kinematical shoulder at 1311 keV.

clearly observed above the other backgrounds. Such a determination would obviate the need to rely on MC for the purpose of determining the concentration of $^{\text{nat}}\text{K}$. Our results indicate that given the background levels from other sources (mainly ^{238}U and ^{232}Th), this shoulder could be observed or a useful upper bound can be obtained. Unfortunately, the DAMA collaboration has not released the spectrum at this energy range. Assuming that the bump at 3 keV is entirely due to background we predict that a shoulder with a height of about 0.04 cpd/kg/keV should be seen at around 700 keV, associated with the β^- decay of ^{40}K .

Finally, a MC simulation is necessary to estimate the rate associated with (iii) where the 1460 keV gamma-ray escapes entirely undetected. This was done independently in Ref. [16] where the total contribution from (i), (ii) and (iii) was taken into account with $\text{BR}_{\text{EC}} = 0.2\%$. In order to investigate the effect of different values of BR_{EC} we subtracted the contribution of (i) and (ii) from the total ^{40}K spectrum quoted in Ref. [16] to obtain the spectrum associated with the EC decay to the excited state, contribution (iii). From Fig. 2 we find that (iii) is indeed the dominant source of ^{40}K background at $E_R \sim 3$ keV by a factor of about $5 \times (0.2/\text{BR}_{\text{EC}})$. Given the importance of this background it would be interesting to compare this number with DAMA-internal MC simulations.

We close this section by noting that the flat spectrum at low energies associated with the 3U transition to ^{40}Ca is a universal feature of β^- decay. In the non-relativistic limit, the product of Fermi function and phase space volume in β^- decay reads,

$$\frac{2\pi\eta}{1 - e^{-2\pi\eta}} \times p^2(E_0 - E)^2 dp \rightarrow \text{const} \times dE \quad (\eta \gg 1),$$

where $\eta = Z\alpha/v$ is the Sommerfeld parameter and v is the asymptotic electron velocity; for β^- decay of ^{40}K , $\eta > 1$ for $E \lesssim 200$ keV and the last equality is approximately constant in this energy regime. We suggest that the essentially flat low-energy event rate seen in DAMA (more than 20 data-points reported up to $E_R \leq 10$ keV and between 20 – 30 keV with negligible error-bar) is strongly suggestive of the presence of such a constant background component (*e.g.* through an unaccounted β^- -emitter or from low-energy Compton background) at a level of⁷

$$B_{\text{flat}} \simeq 0.85 \text{ cpd/kg/keV}. \quad (9)$$

In what follows, we will assume that this is indeed the case and work out the implications for a successful DM interpretation given that potassium is present as well. Hence, $B_0 = B_{\text{flat}} + B_{40}$ where B_{40} is the low-energy background from ^{40}K .

IV. DM SIGNAL INTERPRETATION IN THE PRESENCE OF BACKGROUNDS

We now proceed to investigate the influence of backgrounds on the DAMA DM signal claim. To better quantify the issue let us write $R_0 = B_0 + S_0$ where B_0 is background and S_0 is the unmodulated contribution of any tentative DM signal. These quantities depend on E_R but are assumed to be stationary in time. The total event rate in the presence of a DM signal is then given by⁸

$$R(t) = B_0 + S_0 + S_m \cos \omega(t - t_0). \quad (10)$$

The observed modulating fraction of the event rate has its maximum at a recoil energy of approximately 3 keV, and in the (2 – 4) keV energy bin,

$$s_m^{\text{obs}} = \frac{S_m}{B_0 + S_0} \Big|_{2-4 \text{ keV}} \simeq 2\%. \quad (11)$$

Written in this form, it becomes clear that an understanding of the background B_0 is essential for a successful interpretation of the DAMA results.

A viable DM model must reproduce the observed modulation amplitude, and in particular have sufficiently large modulation amplitude near 3 keV_{ee} recoil energy. Given a certain background level B_0 we have

$$s_m^{\text{max}} \geq \left(1 + \frac{B_0}{S_0}\right) s_m^{\text{obs}} \approx 2\% \times \left(1 + \frac{B_0}{S_0}\right) \quad (12)$$

where $s_m^{\text{max}} \equiv S_m/S_0|_{2-4 \text{ keV}}$ is the maximum modulation fraction. For very low background levels ($B_0/S_0 \ll 1$) the requirement on the signal's modulation amplitude $s_m^{\text{max}} \geq 2\%$ can be easily satisfied by most models of DM that aspire to explain the DAMA result. However, considering the bump around 3 keV in the unmodulated rate, it is almost certainly the case that the background levels are not that low.

Using the background contributions just discussed, including the flat contribution in Eq. (9), we compute the required modulation fraction in (2 – 4) keV from Eq. (12) as a function of both the branching ratio BR_{EC} and the contamination level of $^{\text{nat}}\text{K}$; The unmodulated signal rate, S_0 , is required to explain the observed single hit rate in that bin, $R_0 \simeq 2.2$ cpd/kg. Contours of the required fraction are shown in Fig. 3. Since the contribution from EC into the excited state of ^{40}Ar (case (iii) in the previous section) is obtained from MC and its uncertainty is unknown we consider two scenarios: fractions including this contribution are shown as solid contours whereas fractions neglecting this contribution are shown as dotted contours. In the respective shaded regions s_m^{max} would be larger than 100% and these regions are therefore excluded.

⁷ An extended discussion regarding this hypothesis can be found in an addendum to this paper [18].

⁸ See Ref. [14] for a review and Ref. [19] for a discussion of the general temporal variations expected.

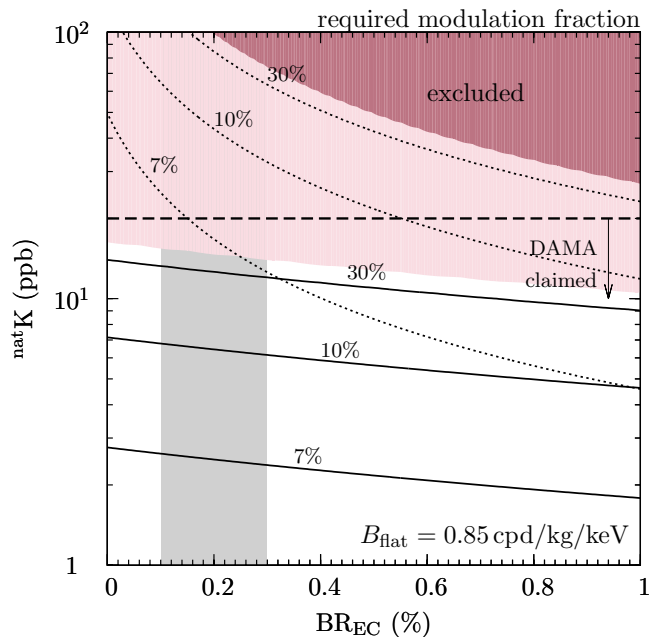


FIG. 3. Required modulating fraction S_m/S_0 of a DM signal at $3 \text{ keV}_{\text{ee}}$ nuclear recoil energy in the presence of a flat background and potassium contamination. Solid (dotted) lines are the associated contours in the parameters BR_{EC} and c_K with (without) background contribution (iii) as detailed in Sec. III. In the (red) shaded regions, the required modulating fraction exceeds 100%. The vertical gray band indicates the nominal value for BR_{EC} and its uncertainty as quoted in Eq. (5). The horizontal dashed line shows the DAMA claimed upper limit on ^{40}K contamination.

As is clear from the figure, any model with small modulation fraction of a few % is already strongly disfavored by the data. Light DM models, which usually predict $\sim 10\%$ modulation fraction (see e.g. [20]), are also in tension with the data. The viability of these models can be better assessed with a measurement of BR_{EC} and a more thorough investigation of the contamination levels from $^{\text{nat}}\text{K}$. Finally, inelastic DM models [21] such as MiDM [22] can yield a large modulation fraction ($\gtrsim 30\%$) due to the heightened sensitivity to the galactic escape velocity. Such models are unlikely to be ruled out through our simple considerations. It is however remarkable that if the DAMA quoted bound on $^{\text{nat}}\text{K}$ is indeed saturated ($c_K = 20 \text{ ppb}$) and the strength of background (iii) is adequately caught by the MC simulation, then the required modulation fraction cannot be attained by any DM model. The necessity of a more comprehensive discussions of backgrounds in the signal region by the DAMA collaboration is evident.

V. COMMENTS ON REALIZING A MEASUREMENT OF THE RARE DECAY OF ^{40}K

Given the above, a direct measurement of the branching ratio of the rare electron capture decay of ^{40}K directly to the ground state of ^{40}Ar is clearly desirable. The very low energy ($\sim 3 \text{ keV}$) released make such a measurement challenging and higher concentrations of ^{40}K compared with the natural abundance is likely needed. It is possible to obtain enriched potassium samples with a ^{40}K concentration of 14% and higher [23]. Such a high concentration would lead to an activity at the level of

$$\sigma_K \approx 380 \text{ day}^{-1} \text{ mg}^{-1} \times (\text{BR}_{\text{EC}}/0.2\%), \quad (13)$$

so that statistics is unlikely to be the limiting factor of any effort to measure BR_{EC} . The main difficulty in measuring the rare decay directly to the ground state is the small branching ratio compared with the more common EC decay $^{40}\text{K} \rightarrow ^{40}\text{Ar}^*(1460)$. As discussed before, if the 1460 keV γ -ray escapes the detector, only the deposition of 3 keV of energy is registered, which mimics the direct decay. However, with an additional surrounding *anti-coincidence* veto, this background becomes reducible. Given that the ratio of branching ratios of the two decays is $\sim 0.2\%/10\% = 2\%$ the veto efficiency only needs to be somewhat better than 1%. Whether this is a realistically attainable efficiency is beyond our expertise to determine.

The low energy release of $\sim 3 \text{ keV}$ is not an easy energy range for detection, but NaI(Tl) crystals such as the ones used by the DAMA collaboration have been demonstrably sensitive in this range. Germanium based detectors such as the ones employed by the CoGeNT collaboration [24] have an even lower threshold and better energy resolution. A precise measurement of the electron capture decay of ^{40}K seems possible. Finally, we note that scintillating crystals can also be grown from KI(Tl) powders and have in fact been used in measurements of the ^{40}K decay scheme [25]. Because of the relatively smaller scintillation light output in comparison with NaI(Tl), it remains to be proven if sensitivity at 3 keV can be attained.

Finally, there has recently been some renewed interest in the exotic possibility of temporal variations in nuclear decay rates [26]. The data used is rather old and suspect, and there has since been several refutations of these claims [27–30]. However, we point out that no conclusive exclusion of such an effect has been reported in the case of EC decay rates.⁹ Thus, it might be of some interest

⁹ Ref. [28] searched for correlation between the Sun-Earth distance to the ratio of $^{22}\text{Na}/^{44}\text{Ti}$. ^{44}Ti decays via EC, whereas ^{22}Na does so only $\approx 10\%$ so in principle this ratio can be sensitive to variations associated with EC. A power-spectrum analysis of the data (which [28] did not perform) seems to reveal significant power at a period of one year and therefore such variations cannot be robustly excluded.

to search for such modulations in the electron capture decay of ^{40}K directly to the ground state of ^{40}Ar . This is especially interesting given the unique nature of this rare decay and its direct relevance to the annual modulations claimed by the DAMA collaboration.

VI. CONCLUSIONS

In this letter we have identified a branch of ^{40}K decay which is yet experimentally unverified and whose strength is only estimated from theory. Aside from its intrinsic importance as the only such known decay of its kind, this branch has important ramifications for DM direct detection. The in-situ presence of ^{40}K is well established in the DAMA detector although the precise contamination level is not clear. Interestingly, it presents a background in the very signal region from where the collaboration derives its claim for DM detection. Before closing we would like to highlight some of our findings:

- The ^{40}K EC decay to the ground state of ^{40}Ar —a third forbidden unique transition and the only one known of its kind—lacks a dedicated measurement to-date.
- Nuclear data evaluations use extrapolations to infer the associated branching. Although we find good agreement when using leading-order theory, a direct experimental verification is nevertheless much desired and called for.
- Depending on the actual concentration of ^{40}K , a DM explanation of the DAMA signal based on elastic scattering and a Maxwellian halo velocity profile may already be excluded.
- With a potassium concentration of 10 ppb (which is below the DAMA inferred upper limit), its β^- decay may very well dominate the spectrum at 1 MeV. The 3U shape with its kinematical shoulder could then be used as an independent measurement of the ^{40}K concentration.

Based on the above findings we propose the following steps to help improve the situation:

- A dedicated measurement of the ^{40}K EC decay into the ground state—potentially over an extended period of time to exclude the possibility of tempo-

ral variations—is itself a missing piece in the experimental verification of leading order weak decay calculations and will help to settle the role of this decay in the DAMA experiment.

- We propose that the concentration levels of $^{\text{nat}}\text{K}$ can be inferred from the activity level associated with the β^- shoulder of ^{40}K at around 1 MeV. This method has been verified impressively in [31] for a NaI prototype crystal by the ANAIS collaboration. A count rate in DAMA much greater than 0.04 cpd/kg/keV will severely undermine a DM interpretation of the signal. This assumes that the other reported concentrations are reliable and that a flat background at a level of 0.85 cpd/kg/keV is present.
- The DAMA spectrum between 10-20 keV should be released as it 1) helps to clarify the hypothesis of a flat β^- backgrounds and 2) potentially allows to identify further EC elements if other K-shell capture “bumps” were present.
- We urge the collaboration to provide more details concerning the probability of coincidence events when the 1460 keV gamma-ray from ^{40}K decay escapes one crystal but is detected elsewhere. A comparison with the independent study by [16] could yield precious insights into the reliability of the MC models and corroborate the determination of $^{\text{nat}}\text{K}$ through the coincidence method.
- Likewise, showing the α -peaks in the spectrum above ~ 2 MeV could reaffirm the average levels of ^{238}U and ^{232}Th determined by DAMA and clarify their contributions to the count rates in the DM signal region.

ACKNOWLEDGMENTS

We acknowledge helpful discussions with K. Blum, A. Chen, R. Lang, V. Kudryavtsev, F. Pröbst and N. Weiner. BS and IY are supported in part by funds from the Natural Sciences and Engineering Research Council (NSERC) of Canada. Research at the Perimeter Institute is supported in part by the Government of Canada through Industry Canada, and by the Province of Ontario through the Ministry of Research and Information (MRI).

[1] X. Mougeot and R. G. Helmer (DDEPWG), (2009), http://www.nucleide.org/DDEP_WG/Nuclides/K-40_tables.pdf.

[2] D. W. Engelkemeir, K. F. Flynn, and L. E. Glendenin, *Physical Review*. **126**, 1818 (1962).

[3] M. Bé, V. Chisté, C. Dulieu, E. Browne, C. Baglin, V. Chechev, N. Kuzmenko, R. Helmer, D. Macmahon, and K. Lee, *Monographie BIPM-5* (2004).

[4] B. Singh, J. L. Rodriguez, S. S. M. Wong, and J. K. Tuli, *Nucl.Data Sheets* **84**, 487 (1998).

[5] ENSDF (ENSDF), <http://www.nndc.bnl.gov/ensdf/>.

- [6] R. Bernabei *et al.* (DAMA Collaboration, LIBRA Collaboration), *Eur.Phys.J.* **C67**, 39 (2010), arXiv:1002.1028 [astro-ph.GA].
- [7] N. B. Gove and M. J. Martin, *Nuclear Data Tables* **10**, 205 (1971).
- [8] W. Bambynek, H. Behrens, M. Chen, B. Crasemann, M. Fitzpatrick, *et al.*, *Rev.Mod.Phys.* **49**, 77 (1977).
- [9] J. P. Davidson, *Phys.Rev.* **82**, 48 (1951).
- [10] LOGFT (ENSDF), http://www.nndc.bnl.gov/nndcscr/ensdf_pgm/analysis/logft/unx/.
- [11] G. G. T. Warburton, E. K. and I. S. Towner, *Annals of Physics* **57**, 174 (1970).
- [12] K. Kossert and E. Gunther, *App. Rad. and Isotop.* **60**, 459464 (2004).
- [13] R. Bernabei *et al.* (DAMA Collaboration), *Nucl.Instrum.Meth.* **A592**, 297 (2008), arXiv:0804.2738 [astro-ph].
- [14] K. Freese, M. Lisanti, and C. Savage, (2012), arXiv:1209.3339 [astro-ph.CO].
- [15] R. Bernabei, P. Belli, F. Cappella, R. Cerulli, C. Dai, *et al.*, *Eur.Phys.J.* **C62**, 327 (2009).
- [16] V. Kudryavtsev, M. Robinson, and N. Spooner, *Astropart.Phys.* **33**, 91 (2010).
- [17] G. Audi, A. Wapstra, and C. Thibault, *Nucl.Phys.* **A729**, 337 (2002).
- [18] J. Pradler and I. Yavin, (2012), arXiv:1210.7548 [hep-ph].
- [19] S. Chang, J. Pradler, and I. Yavin, *Phys.Rev.* **D85**, 063505 (2012), arXiv:1111.4222 [hep-ph].
- [20] J. Kopp, T. Schwetz, and J. Zupan, *JCAP* **1203**, 001 (2012), arXiv:1110.2721 [hep-ph].
- [21] D. Tucker-Smith and N. Weiner, *Phys.Rev.* **D64**, 043502 (2001), arXiv:hep-ph/0101138 [hep-ph].
- [22] S. Chang, N. Weiner, and I. Yavin, *Phys.Rev.* **D82**, 125011 (2010), arXiv:1007.4200 [hep-ph].
- [23] Trace Science International - private communication..
- [24] C. Aalseth *et al.* (CoGeNT Collaboration), *Phys.Rev.Lett.* **101**, 251301 (2008), arXiv:0807.0879 [astro-ph].
- [25] B. Smaller, J. May, and M. Freedman, *Phys. Rev.* **79**, 940 (1950).
- [26] J. H. Jenkins, E. Fischbach, J. B. Buncher, J. T. Gruenwald, D. E. Krause, *et al.*, *Astropart.Phys.* **32**, 42 (2009), arXiv:0808.3283 [astro-ph].
- [27] P. S. Cooper, *Astropart.Phys.* **31**, 267 (2009), arXiv:0809.4248 [astro-ph].
- [28] E. B. Norman, E. Browne, H. A. Shugart, T. H. Joshi, and R. B. Firestone, *Astropart.Phys.* **31**, 135 (2009), arXiv:0810.3265 [astro-ph].
- [29] J. Hardy, J. Goodwin, and V. Iacob, *App.Rad.Isotop.* (2012), 10.1016/j.apradiso.2012.02.021, arXiv:1108.5326 [nucl-ex].
- [30] E. Bellotti, C. Brogгинi, G. Di Carlo, M. Laubenstein, and R. Menegazzo, *Phys.Lett.* **B710**, 114 (2012), arXiv:1202.3662 [nucl-ex].
- [31] S. Cebrian, C. Cuesta, *et al.*, *Astroparticle Physics* **37**, 60 (2012).